

## **OPEN ACCESS**

EDITED BY Hamad Syed, QuBeats, India

REVIEWED BY

Gopala Krishna Podagatlapalli, Gandhi Institute of Technology and Management (GITAM), India Abdul Kalam Shaik, University of Mississippi, United States

\*CORRESPONDENCE
Ben E. Urban,

B benurban@mat.shimane-u.ac.jp

RECEIVED 27 August 2025 REVISED 10 October 2025 ACCEPTED 28 October 2025 PUBLISHED 19 November 2025

### CITATION

Livecchi T and Urban BE (2025) A fiberdelivered, multi-line nanosecond source for single-shot spectro-polarimetric scattering measurements. Adv. Opt. Technol. 14:1693523. doi: 10.3389/aot.2025.1693523

# COPYRIGHT

© 2025 Livecchi and Urban. This is an openaccess article distributed under the terms of the Creative Commons Attribution License (CC BY). The use, distribution or reproduction in other forums is permitted, provided the original author(s) and the copyright owner(s) are credited and that the original publication in this journal is cited, in accordance with accepted academic practice. No use, distribution or reproduction is permitted which does not comply with these terms.

# A fiber-delivered, multi-line nanosecond source for single-shot spectro-polarimetric scattering measurements

Thomas Livecchi<sup>1,2</sup> and Ben E. Urban<sup>3</sup>\*

<sup>1</sup>Optical Imaging Laboratory, Colgate Technology Campus, Piscataway, NJ, United States, <sup>2</sup>Department of Biomedical Engineering, Rutgers University, Piscataway, NJ, United States, <sup>3</sup>Co-Creation Institute for Advanced Materials, Shimane University, Matsue, Japan

We here describe a nanosecond, multi-line laser source that preserves partial linear polarization after transmission through a 100-m large-core graded-index (GRIN) fiber. The system generates narrow emission lines between 473 and 600 nm, evenly spaced by the silica Raman shift of ~440 cm<sup>-1</sup>, from a Q-switched nanosecond pump coupled into the fiber. Despite multimode propagation, the cascaded beams emerge close to diffraction-limited Gaussian profiles due to nonlinear mode self-cleaning, while the residual pump remains multimodal. Across the emission lines, the degree of linear polarization (DoLP) ranges from 0.1 to 0.6 depending on the wavelength. As an application, we demonstrate single-shot, multiwavelength spectropolarimetric reflectance, simultaneously measuring DoLP at all cascaded lines. To our knowledge, this is the first demonstration of wavelength-dependent polarization retention through a 100-m large-core GRIN fiber.

KEYWORDS

fiber laser, polarization-methods, Raman, Gaussian, graded-index fiber

# Introduction

Stimulated Raman scattering (SRS) in optical fibers generates frequency-shifted laser light. The first observations of cascaded Raman scattering in silica fibers date to the 1970s, where successive Stokes shifts produced discrete spectral lines separated by the 440-cm<sup>-1</sup> silica vibrational band (Stolen et al., 1972; Stolen and Ippen, 1973). When the pump intensity exceeds the Raman threshold, additional orders appear sequentially, forming a regularly spaced visible or near-IR spectrum (Liu et al., 2016; Guo et al., 2021).

In graded-index (GRIN) fibers, nonlinear Kerr interactions promote self-cleaning, where multimode inputs evolve toward near-Gaussian outputs despite the large core size (Wright et al., 2016; Krupa et al., 2017; Wabnitz et al., 2018; Niang et al., 2020). On the other hand, maintaining polarization in large-core multimode fibers is challenging. Random intermodal dispersion couples orthogonal polarizations, resulting in polarized inputs being depolarized. Wavefront shaping based on transmission matrix control and adaptive feedback has been used to recover polarization (Popoff et al., 2010; Mosk et al., 2012; Plöschner et al., 2015; Caravaca-Aguirre and Piestun, 2017). Though effective, these approaches are complex, sensitive to perturbations, and unsuitable for moving fiber delivery.

Here, we report that cascade Raman generation in a 100-m large-core GRIN fiber naturally preserves a significant fraction of the linear polarization. Across multiple

generated cascades, the degree of linear polarization (DoLP) remained between 0.1 and 0.6, with wavelength and alignment dependence, along with occasional anomalous behavior. This partial polarization retention, which was not previously reported in large-core GRIN fibers, arises directly from nonlinear mode dynamics and self-cleaning during Raman cascading. Combined with discrete multiline radiation and near-diffraction-limited profiles, partial polarization retention enables single-shot spectro-polarimetric measurements with a compact, fiber-delivered source. We demonstrate this capability using scattering phantoms, where wavelength-dependent DoLP shows both the strength of scattering and superficial sensitivity through polarization memory effects (Krupa et al., 2017; Dark and Kim, 2017).

# Materials and methods

# Optical setup

A Q-switched 473-nm pump laser (Bright Microlaser, SB1-473-3-5) with a pulse width of 1.7 ns, 5 kHz repetition, and  $\sim$ 3  $\mu$ J per pulse was coupled into a large-core (core/cladding = 50/ 125 µm) GRIN fiber (Thorlabs, GIF50C) with a length of 100 m. The laser output was directed onto two silver mirrors mounted kinematically to control the beam position in X and Y. At the back aperture of the objective, the beam size was approximately 3.5 mm ×1.5 mm, so the full numerical aperture (NA) of the objective was not used for focusing but instead for adjusting the launch angle into the fiber. The beam was then directed into the back aperture of a long working distance objective lens (Mitutoyo, 378-803-3), which was mounted in an XY-controllable kinematic mount to enable fine adjustment of the launch angle. The objective focused the beam into the large-core fiber, which was secured in a temporary FC/PC terminator and mounted on a z-stage for axial alignment.

# Raman threshold characterization

The onset of cascade lines was measured by varying the average pump power from 2 to 12 mW (0.4  $\mu J{-}2.4~\mu J{)}$ ). The corresponding pulse energy for the pump laser was calculated using the known 5-kHz repetition rate and 1.7-ns pulse width. The first cascade line appears at an average power of approximately 2.1 mW (0.42  $\mu J{)}$ , demonstrating the intensity-dependent cascade process.

# Beam profiles

Each emission line was first collimated using an output fiber collimator. The collimated lines were then spectrally isolated using a series of narrow bandpass filters. The isolated spectral line was confirmed using a spectrometer before the line was incident on a CMOS camera (Thorlabs, CS505MUP1), where a single image was captured (5 ms integration time, 10 averages). The resulting image was used for Gaussian measurements. An intensity line profile was drawn through the center of the intensity spot and plotted to show the intensity profile of the beam.

# Temporal pulse width measurements

A fast photodiode (Thorlabs, DET025AFC, 2 GHz bandwidth) in combination with an oscilloscope (Tektronix, MDO4104C) was used to measure the temporal pulse width. The output of the fiber was first separated into different wavelengths using a transmission gating (Thorlabs, GT25-06V). After separation, each diffracted individual line was measured using the fast photodiode to show the apparent negative chirp of the output wavelengths.

# Polarization and stability measurements

The fiber output was analyzed using a rotating polarizer (Thorlabs, GTH10M-A) and a fiber-coupled spectrometer (Ocean Insight, USB4000). For each wavelength, the intensity was recorded as the polarizer was rotated from  $0^{\circ}$  to  $360^{\circ}$  in  $10^{\circ}$  steps to determine the polarization modulation. The DoLP was calculated as  $DoLP = I_{max} - I_{min}/I_{max} + I_{min}$ , where  $I_{max}$  and  $I_{min}$  are the extrema of transmitted intensity *versus* analyzer angle. Spectra were acquired through an integrating sphere at each rotation step, and the measurement sequence was repeated every minute over a 30-min interval to evaluate the temporal stability and modal drift. Input polarization measurements were conducted in a similar manner, where a second polarizer (Thorlabs, GTH10M-A) was placed after the laser and rotated in  $5^{\circ}$  increments from  $0^{\circ}$  to  $25^{\circ}$ .

# Bend-radius dependence

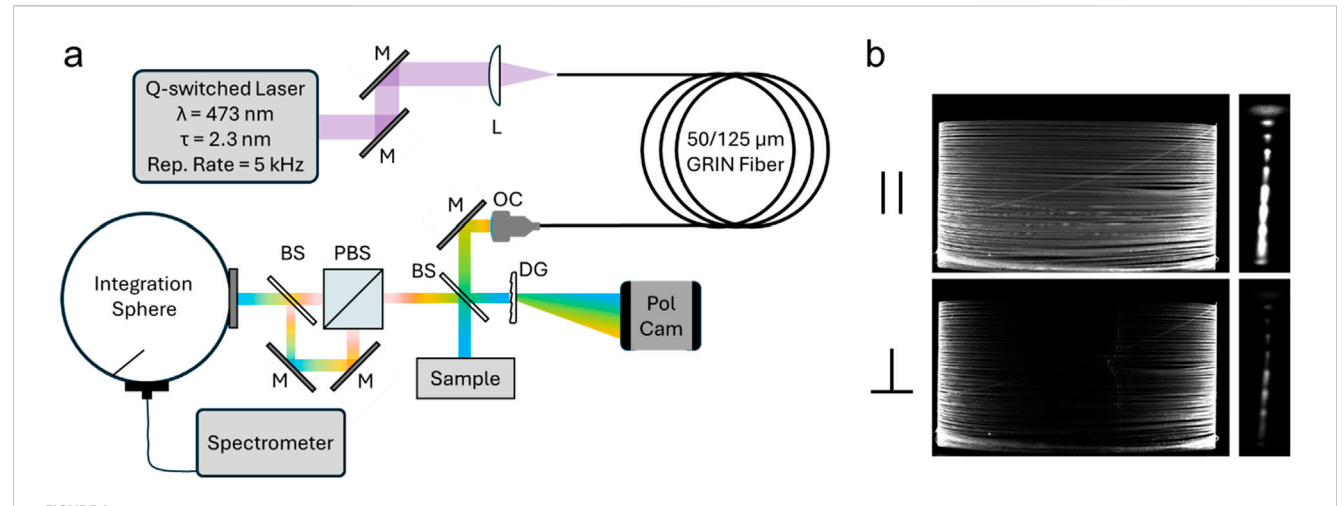
A 5-m section of the GRIN fiber was coiled around spools of 7.5 cm and 4.25 cm radii. DoLP and spectral intensity were measured using a spectrometer for each radius to quantify polarization sensitivity to bending.

# Launch-angle dependence

The launch angle was varied between 0° and 4° to examine the coupling effects on the spectral intensity and polarization stability. The angle was controlled by adjusting the height of the incident pump beam using two mirrors and underfilling the back aperture of the coupling lens.

# Spectro-polarimetric reflectance experiment

Figure 1a shows the illumination setup used to measure wavelength-resolved co- and cross-polarized backscatter and to derive DoLP and the retention  $R = \frac{(DoLP_{out})}{(DoLP_{in})}$ . The collimated output from the GRIN fiber was sent through a 50:50 non-polarizing beamsplitter (BS) to illuminate the intralipid surface at normal incidence. Light directly reflected from the BS was sent through a low polarization sensitivity transmission-type diffraction grating (Edmund Optics, 49-579) before being incident on the polarization camera. An absorption-type neutral density filter (Thorlabs, NE40B) was used to reduce laser light on the camera.



(a) Simplified optical schematic. A 473-nm pulsed pump is coupled into a 100-m GRIN fiber (M, mirror; L, lens). The output is collimated using an output fiber collimator (OC) and directed onto a beamsplitter (BS). Half of the split light is sent through a transmission diffraction grating (DG) before being incident on a polarization camera. The other half is incident on the sample in an epi-reflection setup. Light backscattered by the sample is again incident off the BS and sent into a polarizing beam splitter (PBS), which separates co- and cross-polarization light. The two polarization paths are recombined using another BS, which also directs light into an integrating sphere attached with an optical fiber to a spectrometer. Light is blocked from one arm for each polarization measurement. (b) Polarization-camera images of the GRIN fiber spool (left) and first-order diffraction of the transmission grating (DG) (right), which were measured as shown in (a). The top point in the diffraction image is the fundamental beam.

Backscattered light returned through the same BS and was separated by a polarizing BS (PBS, Thorlabs PBS201) into co- and crosschannels defined with respect to the launch polarization. Each channel passed through matched relay optics and was recombined with a second 50:50 BS, so both polarizations shared the same optical path into an integrating sphere (Newport 819C-SL-5.3-CAL2). A 400-um multimode fiber coupled the sphere output to a spectrometer (Ocean Insight, USB4000). Co- and cross-spectra were recorded in two sequential exposures by alternately shuttering the unused PBS arm; this ensured identical optics and detector response for both channels. Prior to phantom measurements, a silver mirror replaced the sample to calibrate  $DoLP_{in}$  and determine scalar correction factors for small S/P imbalances from the recombination BS. Intralipid suspensions (0.5%, 1.0%, and 1.5% in water) served as scattering phantoms. Only the six cascaded lines with input DoLP >0.10 were analyzed.

# Results

Images of the GRIN fiber output recorded with a polarization camera showed distinct polarization contrast, indicating that light escaping the fiber maintains a preferential polarization through the length of the fiber (Figure 1b, left). Diffraction through the transmission grating produced spectrally separated spots, dominated by co-polarized components, confirming partial polarization preservation across the cascades (Figure 1b, right).

Figure 2 shows the spectral characteristics of the cascade emission. Launch alignment yielded distinct spectral distributions, which demonstrate the mode-selective gain (Figure 2, left). The stability of each peak was also measured (Figure 2, right). The stability had a relation to the launch alignment. Normal incidence (0°) showed the most stability but also produced the least cascades for the constant pump energy.

Intensity line profiles confirmed that the cascade beams, except for the pump, were mostly Gaussian in shape (Figure 3). Although the pump beam was 1.7 ns, cascaded beams exhibited a negative chirp of hundreds of picoseconds to more than a nanosecond.

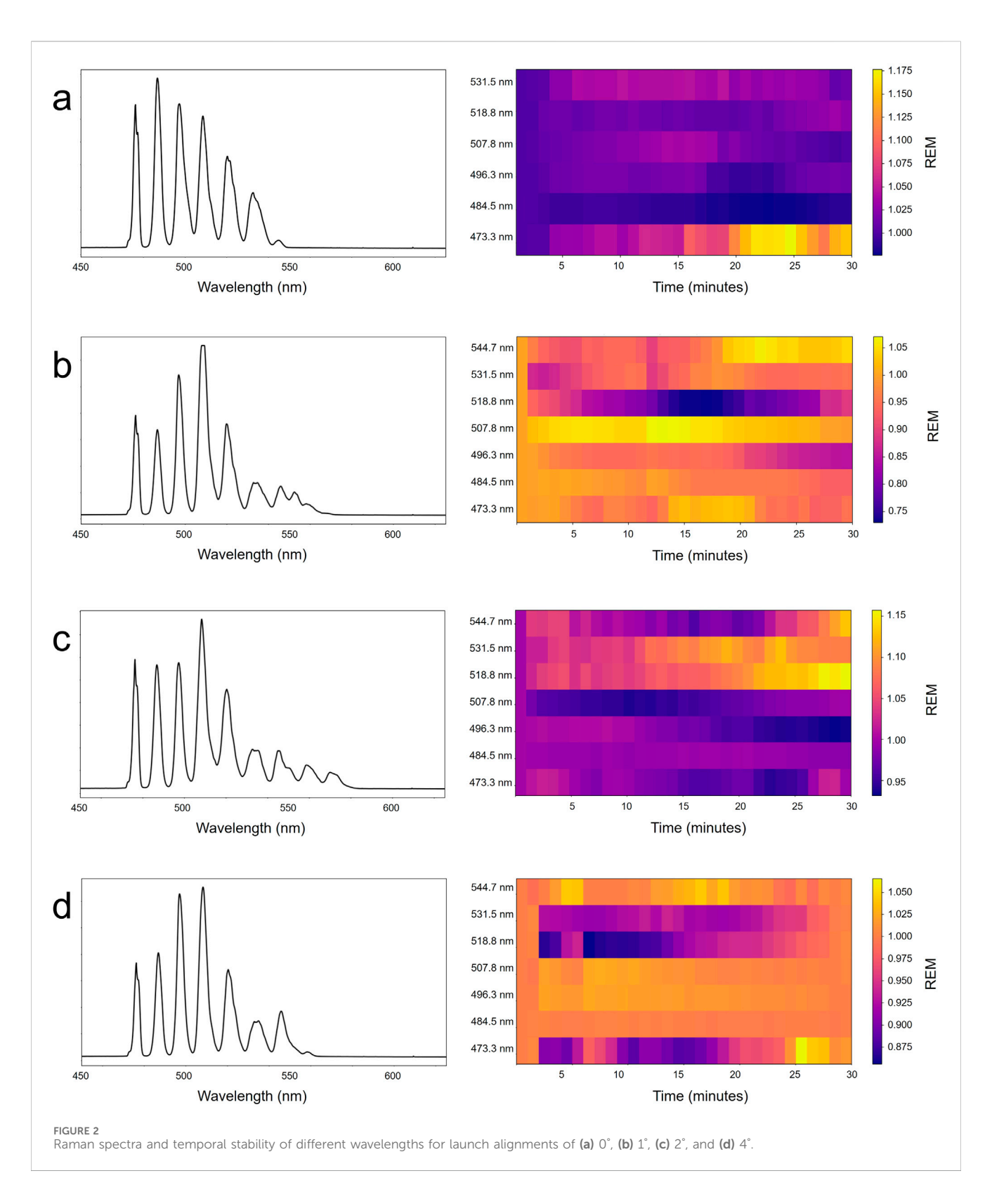
The average power-dependent threshold for the first Raman line was approximately 2.1 mW (0.42  $\mu$ J per pulse). Above this threshold, the number and width of Stokes lines increased with input power and alignment (Supplementary Figure S1).

Polarization measurements confirmed that the cascaded beams retained partial polarization, with DoLP values between 0.1 and 0.6 depending on the wavelength. The polarization DoLP was not monotonic across the generated wavelengths. Alignment influenced the observed DoLP and polarization (Supplementary Figure S2), with the 531.5 nm and 544.7 nm lines occasionally showing little or reversed polarization relative to the other cascade line polarization. Bend-radius and polarization-angle experiments showed that these anomalies correspond with local modal coupling and birefringence variations (Supplementary Figure S3, 4).

To demonstrate an application of the laser, spectro-polarimetric reflectance experiments with intralipid phantoms were performed. We measured the polarization retention with wavelength,  $R(\lambda) = DoLP_{out}/DoLP_{in}$ , for the scattering samples. Only lines with DoLP values greater than 0.1 were used for the scattering experiments. The scattering experiments revealed that DoLP decreased with increasing scatterer concentration (Figure 4). The experiments were repeated five times, and the standard error of the mean was considered in the results.

# Discussion

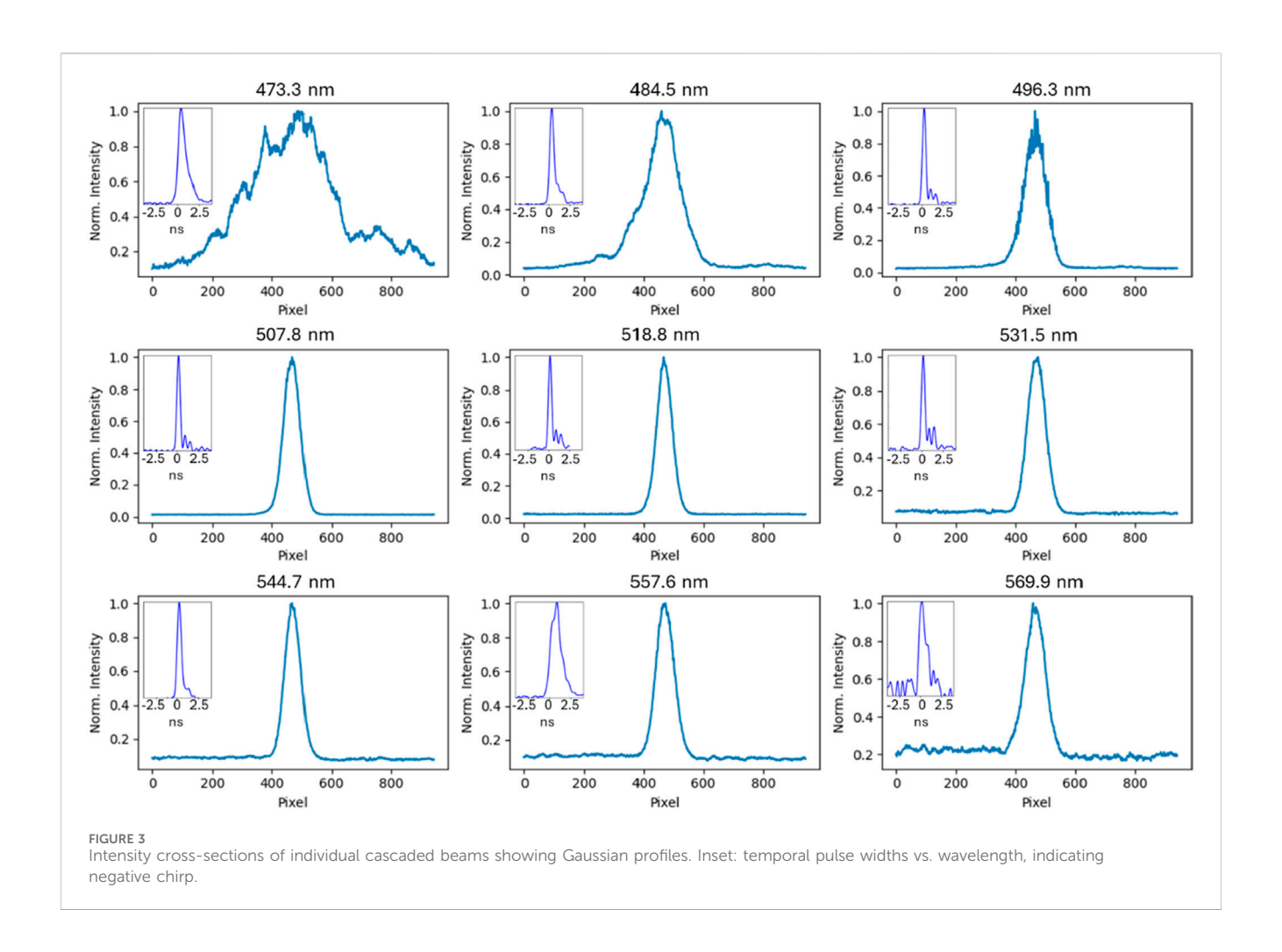
The pump laser with the large-core GRIN fiber produced multiline nanosecond emission that retained partial polarization

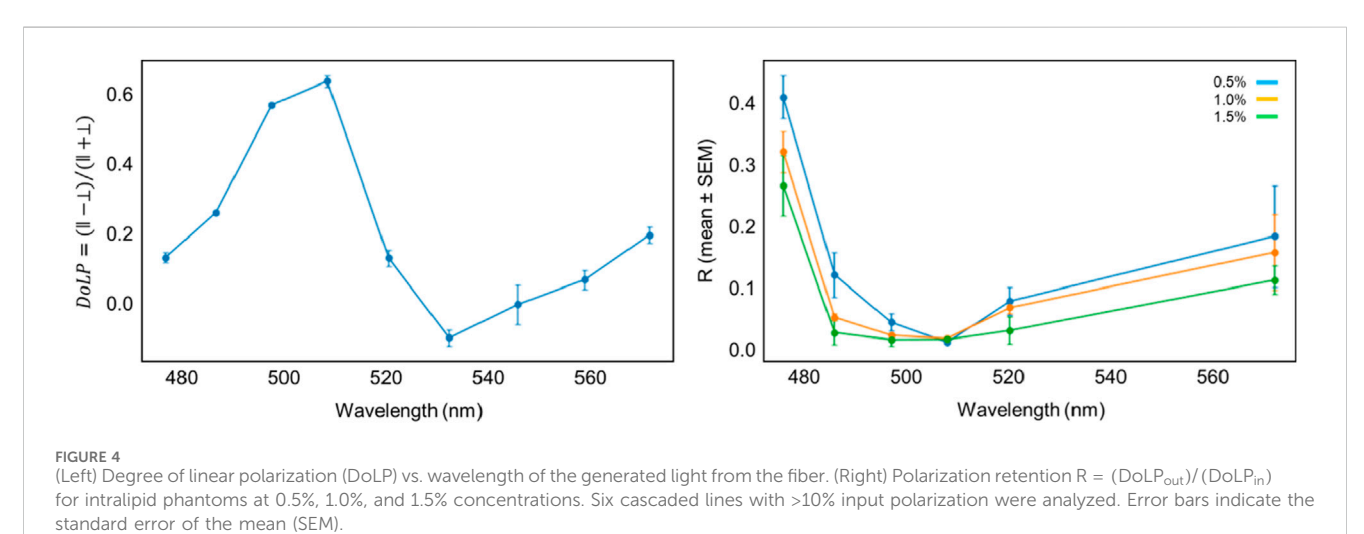


after 100 m of propagation. DoLP values of 0.1–0.6 were observed across most emission lines, demonstrating stable polarization retention in a large-core multimode fiber at the same polarization as the pump laser. All cascaded output radiation was near-Gaussian, while the output of the pump remained multimodal. In addition, the cascaded lines showed negative chirp, with pulse

widths shorter by hundreds of picoseconds compared to that of the 1.7 ns pump.

At the applied peak powers, both Raman gain and self-phase modulation shaped the spectral evolution. Raman amplification set the center frequencies and spacing of the cascade, while the full width at half maximum (FWHM) of successive





Stokes lines broadened from approximately 3 nm for the pump to more than 8 nm for higher orders. This steady broadening shows that nonlinear phase accumulation and group-velocity dispersion in the 100-m fiber add temporal chirp and spectral width beyond the intrinsic Raman linewidth. Raman gain governs the wavelength positions and

conversion efficiency, while SPM and GVD define the spectral envelopes.

The results implicate several nonlinear effects. Nonlinear Kerr interactions in GRIN fibers promote beam self-cleaning, preferentially transferring energy into low-order modes that maintain Gaussian profiles and more stable polarization (Wright

et al., 2016; Krupa et al., 2017; Wabnitz et al., 2018; Niang et al., 2020; Krupa et al., 2019). Consequently, stimulated Raman scattering favors these modes (Xu et al., 2017; Liu et al., 2016). Thus, cascaded lines are diffraction-limited, while the depleted pump remains multimodal.

Launch conditions determine the relative efficiency of each order, allowing tuning the intensity and polarization between lower- and higher-order Stokes lines (Liu et al., 2023). In our measurements, the DoLP distribution was nonmonotonic, with intermediate orders exhibiting the strongest polarization while others showed reduced or negligible polarization. The alignment-dependent inversion of polarization and loss of polarization at 531.5 nm and 544.7 nm suggest that wavelength-dependent intermodal coupling and local birefringence changes can rotate or scramble the polarization axis for specific Raman orders. Therefore, the polarization properties of individual lines reflect Kerr-driven self-cleaning, order-specific modal gain, and coupling conditions.

Maintaining polarization in multimode fibers is difficult because random intermodal dispersion couples orthogonal states and depolarizes the output (Caravaca-Aguirre and Piestun, 2017; Mosk et al., 2012; Plöschner et al., 2015; Popoff et al., 2010). Wavefront-shaping methods based on transmission-matrix measurement and adaptive feedback can restore polarization at the distal end (Caravaca-Aguirre and Piestun, 2017; Mosk et al., 2012), but they are complex, require stability, and are impractical for moving fiber systems. The present results show that GRIN fibers can retain a useful level of polarization without active control when Raman cascading and Kerr self-cleaning occur.

The phantom scattering experiments show that DoLP decreases with scattering concentration, which is in agreement with the polarization-memory theory in turbid media (Dark and Kim, 2017). The suppression observed for higher scattering concentrations highlights sensitivity to the mean free path of travel. Additionally, R recovered slightly at longer wavelengths. This is likely due to the remaining casein micelles in the lipid phantoms after centrifuging from milk. The casein micelles have a scattering cross-section that varies with the wavelength (Stocker et al., 2017).

These results demonstrate that a GRIN-fiber Raman cascade laser provides discrete multi-line emission, nanosecond pulses with negative chirp, partial polarization retention, and diffraction-limited output suitable for depth-sensitive spectroscopy and scattering studies.

# Conclusion

We demonstrated a GRIN-fiber Raman cascade laser that produces discrete multi-line visible emission, nanosecond pulses with negative chirp, near-Gaussian spatial quality, and wavelength-dependent partial polarization retention. Using this source, we performed the first single-shot, multiwavelength spectro-polarimetric reflectance measurements with a fiber-delivered system. The measurements revealed scattering-dependent polarization memory and anomalous polarization behavior linked to mode coupling in specific Raman orders. This work establishes new opportunities for versatile, low-cost multiline sources in biomedical spectroscopy and polarization-based scattering studies.

# Data availability statement

The raw data supporting the conclusions of this article will be made available by the authors on reasonable request.

# Author contributions

TL: Data curation, Formal Analysis, Investigation, Visualization, Writing – original draft, Writing – review and editing. BU: Conceptualization, Data curation, Formal Analysis, Funding acquisition, Investigation, Methodology, Project administration, Resources, Software, Supervision, Validation, Visualization, Writing – original draft, Writing – review and editing.

# **Funding**

The authors declare that financial support was received for the research and/or publication of this article. This project was funded by Colgate-Palmolive, Piscataway, NJ, USA. The funder was not involved in the study design, collection, analysis, interpretation of data, the writing of this article, or the decision to submit it for publication.

# Conflict of interest

The authors declare that the research was conducted in the absence of any commercial or financial relationships that could be construed as a potential conflict of interest.

# Generative AI statement

The authors declare that Generative AI was used in the creation of this manuscript. Generative AI was used in the article to check for spelling errors and sentence clarity.

Any alternative text (alt text) provided alongside figures in this article has been generated by Frontiers with the support of artificial intelligence and reasonable efforts have been made to ensure accuracy, including review by the authors wherever possible. If you identify any issues, please contact us.

# Publisher's note

All claims expressed in this article are solely those of the authors and do not necessarily represent those of their affiliated organizations, or those of the publisher, the editors and the reviewers. Any product that may be evaluated in this article, or claim that may be made by its manufacturer, is not guaranteed or endorsed by the publisher.

# Supplementary material

The Supplementary Material for this article can be found online at: https://www.frontiersin.org/articles/10.3389/aot.2025.1693523/full#supplementary-material

# References

Caravaca-Aguirre, A. M., and Piestun, R. (2017). Single multimode fiber endoscope.  $Opt.\ express\ 25$  (3), 1656–1665. doi:10.1364/oe.25.001656

Dark, J. P., and Kim, A. D. (2017). Asymptotic theory of circular polarization memory. J. Opt. Soc. Am. A 34, 1642–1650. doi:10.1364/JOSAA.34.001642

Guo, X., Li, Z., Jiao, Y., Zhao, Z., Yao, C., Jia, Z., et al. (2021). A shower of mid-infrared Raman solitons at designed wavelength of  $\sim$ 3  $\mu$ m from a tapered fluorotellurite fiber. Laser Phy. 31 (9), 095103. doi:10.1088/1555-6611/ac1607

Krupa, K., Tonello, A., Shalaby, B. M., Fabert, M., Barthélémy, A., Millot, G., et al. (2017). Spatial beam self-cleaning in multimode fibres. *Nat. Photonics* 11, 237–241. doi:10.1038/nphoton.2017.32

Krupa, K., Tonello, A., Barthélémy, A., Mansuryan, T., Couderc, V., Millot, G., et al. (2019). Multimode nonlinear fiber optics, a spatiotemporal avenue. *Apl. Photonics* 4, 110901. doi:10.1063/1.5119434

Liu, Z., Wright, L. G., Christodoulides, D. N., and Wise, F. W. (2016). Kerr self-cleaning of femtosecond-pulsed beams in graded-index multimode fiber. *Opt. Lett.* 41, 3675–3678. doi:10.1364/OL.41.003675

Liu, J., Liang, H., Wang, Q., Gao, S., Zhang, H., and Chen, J. (2023). Random Yb-fiber laser with intracavity raman frequency-comb generation. *High. Power Laser Sci. Eng.* 11, e11. doi:10.1017/hpl.2022.40

Mosk, A. P., Lagendijk, A., Lerosey, G., and Fink, M. (2012). Controlling waves in space and time for imaging and focusing in complex media. *Nat. Photonics* 6, 283–292. doi:10.1038/nphoton.2012.88

Niang, A. O., Jima, M. A., Modotto, D., Mangini, F., Tonello, A., Minoni, U., et al. (2020). Spatial beam self-cleaning in tapered Yb-doped GRIN multimode fiber with

decelerating nonlinearity. SPIE Proc. 11665, 86–93. doi:10.1109/JPHOT.2020. 2979938

Plöschner, M., Tyc, T., and Čižmár, T. (2015). Seeing through chaos in multimode fibres. *Nat. Photonics* 9, 529–535. doi:10.1038/nphoton.2015.112

Popoff, S. M., Lerosey, G., Carminati, R., Fink, M., Boccara, A. C., and Gigan, S. (2010). Measuring the transmission matrix in optics: an approach to the study and control of light propagation in disordered media. *Phys. Rev. Lett.* 104, 100601. doi:10. 1103/PhysRevLett.104.100601

Stocker, S., Foschum, F., Krauter, P., Bergmann, F., Hohmann, A., Scalfi Happ, C., et al. (2017). Broadband optical properties of milk. *Appl. Spectrosc.* 71 (5), 951–962. doi:10.1177/0003702816666289

Stolen, R. H., and Ippen, E. P. (1973). Raman gain in glass optical waveguides. *Appl. Phys. Lett.* 22 (6), 276–278. doi:10.1063/1.1654637

Stolen, R. H., Ippen, E. P., and Tynes, A. R. (1972). Raman oscillation in glass optical waveguide. *Appl. Phys. Lett.* 20, 62–64. doi:10.1063/1.1654046

Wabnitz, S., Tonello, A., Couderc, V., Modotto, D., Barthélémy, A., Millot, G., et al. (2018). Nonlinear dynamics in multimode optical fibers. *Present. Quantum Sens. Nano Electron. Photonics XV*, SPIE Proc. 10540, 290–296.

Wright, L. G., Liu, Z., Nolan, D. A., Li, M.-J., Christodoulides, D. N., and Wise, F. W. (2016). Self-organized instability in graded-index multimode fibres. *Nat. Photonics* 10, 771–776. doi:10.1038/nphoton.2016.227

Xu, L., Chen, R., Ma, C., Yang, S., and Wang, L. V. (2017). Raman-shifted wavelength-selectable pulsed fiber laser for photoacoustic microscopy in the visible range. *Opt. Express* 25, 351–356. doi:10.1364/OE.25.000351